Adsorption of Single and Multiple Graphene-Oxide Nanoparticles at a Water-Vapor Interface

Gravelle, Simon; Botto, Lorenzo

DOI
10.1021/acs.langmuir.1c01902

Publication date
2021

Document Version
Final published version

Published in
Langmuir

LANGMUIR

pubs.acs.org/Langmuir Article

Adsorption of Single and Multiple Graphene-Oxide Nanoparticles at a Water−Vapor Interface

Simon Gravelle and Lorenzo Botto*

Cite This: *Langmuir* 2021, 37, 13322−13330 Read Online

ACCESS | Metrics & More | Article Recommendations | Supporting Information

ABSTRACT: The adsorption of graphene-oxide (GO) nanoparticles at the interface between water and vapor was analyzed using all-atom molecular simulations for single and multiple particles. For a single GO particle, our results indicate that the adsorption energy does not scale linearly with the surface coverage of oxygen groups, unlike typically assumed for Janus colloids. Our results also show that the surface activity of the particle depends on the number of surface oxygen groups as well as on their distribution: for a given number of oxygen groups, a GO particle with a patched surface was found to be more surface active than a particle with evenly distributed groups. Then, to understand what sets the thickness of GO layers at interfaces, the adsorption energy of a test GO particle was measured in the presence of multiple GO particles already adsorbed at the interface. Our results indicate that in the case of high degree of oxidation, particle−particle interactions at the water−vapor interface hinder the adsorption of the test particle. In the case of a low degree of oxidation, however, clustering and stacking of GO particles dominate the adsorption behavior, and particle−particle interactions favor the adsorption of the test particle. These results highlight the complexity of multiple particle adsorption and the limitations of single-particle adsorption models when applied to GO at a relatively high surface concentration.

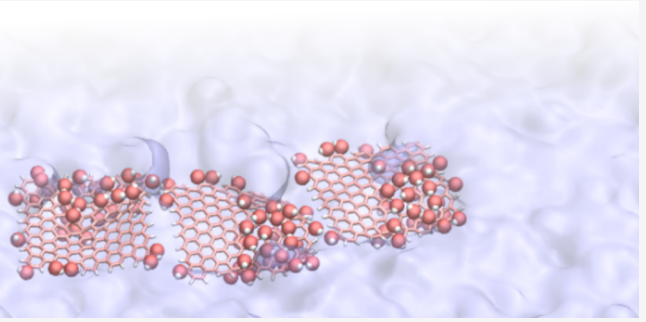

1. INTRODUCTION

The adsorption of micro- and nanoparticles at the interface between two immiscible fluids alters interfacial properties such as surface tension and surface elasticity.[1] This effect is exploited to enhance the stability of emulsions and foams, with applications for the food and cosmetic industries.[2−4] Adsorption at fluid interfaces has also been used to assemble particles into nonplanar configurations, and thus interfaces can serve as a template of functional composite materials and hierarchically structured porous materials,[5−7] as well as clusters, strings, networks, monolayers, and bilayers.[8] Colloidal or molecular particles remain trapped at a fluid−fluid interface if the total interfacial energy of such configuration is smaller than when the particles are in either of the bulk fluids, which can be gases or liquids.[9] The adsorption of spherical and chemically homogeneous particles has been extensively studied,[1] but new investigations show that chemically or geometrically anisotropic particles attach even more strongly to interfaces than their isotropic counterparts.[10,11] Most investigations to date consider single particles. However, the surface concentration is inherently high when effects on interfacial rheology are the most useful. Therefore, it is crucial to extend the current investigations to anisotropic and heterogeneous particles particularly in the limit where particle−particle contacts play a role.

A promising surface-active particle that is both geometrically anisotropic and chemically nonhomogeneous is graphene oxide (GO).[12] GO is an atomically thin nanomaterial similar to graphene but made of carbon atoms that are functionalized with oxygen-containing groups. Its surface presents irregular chemical patches with nanometric lateral extent; hydroxyl and epoxide groups are mostly located at the basal plane and carboxyl groups at the edges.[13] The oxygen groups at the basal plane are typically distributed as islands, resulting in hydrophilic (oxidized area) and hydrophobic (unoxidized graphitic area) nanopatches.[14−17] Such surface heterogeneities contribute to the propensity of GO to adhere to fluid interfaces. For instance, GO has the ability to adsorb at water−air, water−oil, and multiple polymeric interfaces.[18−22] Chemically nonhomogeneous particles are known to adsorb even more strongly to fluid interfaces than homogeneous particles having the same geometry, so there is a need to understand the link between the surface heterogeneities at the surface of GO and

Received: July 16, 2021
Revised: October 4, 2021
Published: November 1, 2021

https://doi.org/10.1021/acs.langmuir.1c01902
Langmuir 2021, 37, 13322−13330

its surface activity.[4] This link is expected to be a complex function of the area-averaged surface coverage of hydrophilic/hydrophobic patches and the distribution of oxygen groups at the particle surface. Therefore, GO particles differ from classical "Janus" particles, where the geometry of the imposed surface heterogeneity is comparatively simple.[10]

Experimental and numerical studies have identified several factors influencing the surface activity of GO: the size of the sheets, with smaller sheets being more hydrophilic due to a larger edge-to-plane ratio;[23] the pH of the solution, with high pH values correlating with more charged and more hydrophilic GO sheets;[19,24] the number of oxygen groups at the basal plane, with particles with a high degree of basal oxidation being too hydrophilic to attach at interfaces, and particles with a low degree of oxidation being surface active.[24,25] Despite recent progress, several fundamental questions concerning the surface activity of GO remain unanswered. Most importantly, the role of the oxygen groups' distribution at the basal surface of GO has not yet been addressed as far as we know. Furthermore, the effect of neighboring particles on adsorption needs to be addressed, as single-particle studies can only shed light on the initial process of adsorption, when the fluid interface is essentially bare. Understanding multiparticle effects can also give insights into the mechanisms that set the thickness of adsorbed GO layers, which ultimately is a key requirement to create GO-based three-dimensional (3D) macroporous materials with predefined structural integrity and barrier properties.[9] Finally, the most desirable effects on interfacial rheology occur when the surface concentration is high and particle−particle interference cannot be ruled out.

In this article, we compute the adsorption energy of single and multiple GO nanoparticles at a water−vapor interface using all-atom molecular dynamics (MD). We first consider the case of a single GO particle, and measure the adsorption energy for varying degrees of oxidation and varying surface distribution of oxygen groups. Then, we consider the case of multiple GO particles and measure the adsorption energy of a test GO particle in the presence of a number N of GO particles at the fluid interface. The article ends with a discussion of the implications of our results and the advantages and limitations of all-atoms molecular simulations for the study of the adsorption of multiple GO particles.

2. MODELS AND METHODS

Simulations were performed using the Large-scale Atomic/Molecular Massively Parallel Simulator (LAMMPS).[26] The system is made of one or more GO particles and a layer of water in a rectangular box with periodic boundary conditions. In all simulations, the layer of water extends periodically in transverse directions (x and y) and has two liquid−vapor interfaces (Figure 1a). The SPC/e water model was used for water,[27] and the all-atom optimized potentials for liquid simulation (OPLS-AA) forcefield was used for GO particles.[28] Crossed parameters for Lennard-Jones interactions were calculated using the Lorentz−Berthelot mixing rule. A temperature T = 300 K was maintained using a Berendsen thermostat. Water molecules were kept rigid with the SHAKE algorithm.[29] Long-range Coulombic interactions were computed using the particle−particle particle−mesh (PPPM) method.[30,31] A time step of 1 fs was used.

2.1. GO Particle. GO particles were built using MakeGraphitics, a software that allows to generate graphene-oxide nanostructures with hydrophilic and hydrophobic nanopatches that are consistent with experiments.[32] Each GO particle was made of a square, atomically thin array of carbon atoms with dimensions 2 nm × 2 nm (Figure 1). Carbon atoms were separated into edges and basal groups (Figure S1). A fraction of edge carbon atoms were functionalized with oxygen-based groups (Figure 1b,c). The edge carbon atoms not functionalized with oxygen-based groups were terminated by hydrogen atoms (hydrogen-terminated graphene edges are known to be energetically more stable than bare graphene edges[33]). We define r_{OH} as the ratio between oxygen-terminated and hydrogen-terminated edge carbon atoms. In addition, a fraction of basal carbon atoms were functionalized with oxygen-based groups. We define the oxygen-over-carbon ratio r_{OC} as the ratio between the oxygen atoms at the basal plane, and the carbon atoms of the basal plane. Unless specified otherwise, only hydroxyl groups were used for the functionalization of the GO particle. GO particles are typically functionalized with three types of group: hydroxyl, epoxide, and carboxyl.[13] Here, for the sake of simplicity and to develop a systematic study, we choose GO particles functionalized only with hydroxyl groups, which considerably reduces the parameter space and makes the quantification of the effect of group distribution and density on the adsorption energy of GO particles less challenging. A comparison of adsorption energy values obtained with single GO particles built with epoxide and carboxyl groups, respectively, is given at the end of Section 2.

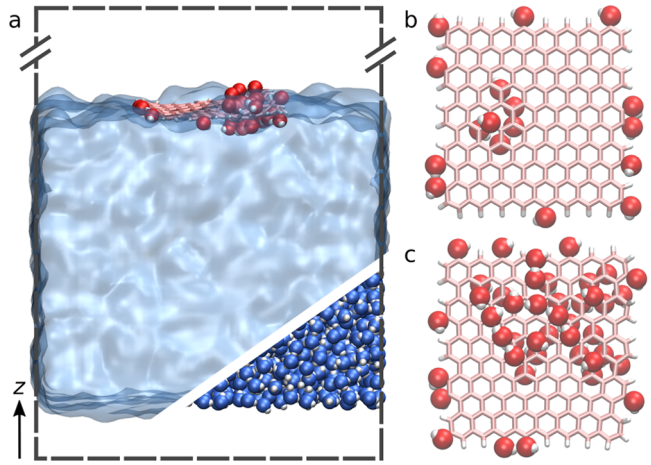

Figure 1. (a) Snapshot of the molecular dynamics system with water in clear blue and a single GO particle with carbon, oxygen, and hydrogen atoms, respectively, in pink, red, and white. Water is represented as a transparent continuum field for clarity, except on the bottom right part where the oxygen and hydrogen atoms of water molecules are shown as blue and white spheres, respectively. Periodic boundary conditions are applied along the black dashed line. (b, c) GO particles for two different degrees of basal plane oxidation, respectively, r_{OC} = 0.05 (b) and r_{OC} = 0.32 (c). In both cases, the degree of edge oxidation is r_{OH} = 0.3, and particles have a square shape with lateral size for the carbon layer equal to 2 nm. The pink hexagonal lattice represents the carbon layer, the red spheres are oxygen atoms, and white spheres are hydrogen atoms.

2.2. Single GO Particle Simulation. In the case of single GO particle simulations, the system consists of a slab of liquid water with a number N_w = 4500 of water molecules in a box of dimensions $L_x \times L_y \times L_z$ = 5.4 × 5.4 × 10 nm^3 and of a single GO particle (Figure 1). The potential of mean force (PMF) corresponding to the free energy along a chosen coordinate was calculated using the umbrella sampling (US) method together with the Weighted-Histogram Analysis Method (WHAM).[34,35] US is a biased molecular dynamics (MD) method, or enhanced-sampling algorithm, that allows to explore the equilibrium states of adsorption without simulating the natural progression of a GO particle exchanging from bulk water to the interface. US was preferred to standard MD because the exchanges of a GO particle between the interface and the bulk can be extremely rare events, due to the relatively large typical adsorption energy expected for these nanometric particles, $\Delta E_{ads} \approx -10\ k_B T$,[24,25] where the adsorption energy is defined as the difference in energy between the particle being in bulk and the particle being at the interface. In the present work, restraints were applied at specific positions z_0 along the axis z to

https://doi.org/10.1021/acs.langmuir.1c01902
Langmuir 2021, 37, 13322−13330

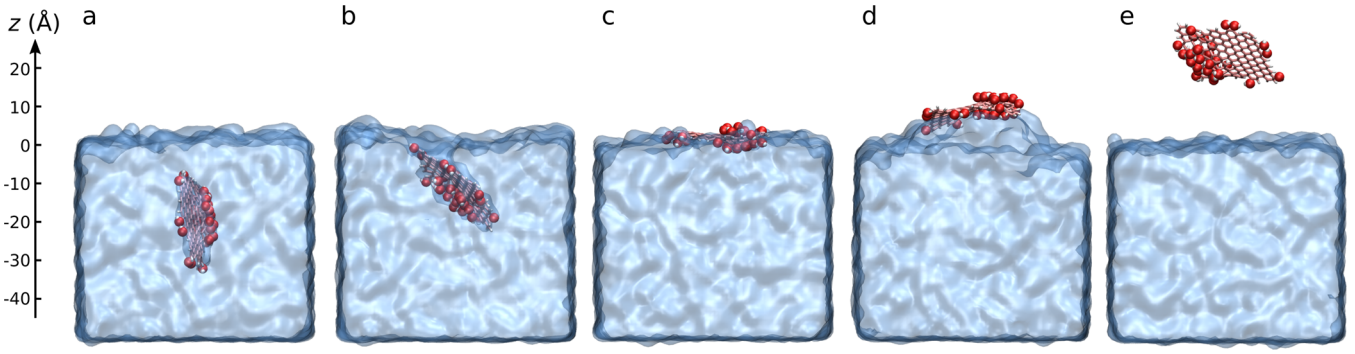

Figure 2. Molecular configuration for five different values of z_0, with, respectively, $z_0 = -20$ Å (a), $z_0 = -10$ Å (b), $z_0 = 0$ Å (c), $z_0 = 10$ Å (d), and $z_0 = 20$ Å (e). Water is represented as a transparent continuum field for clarity.

sample all relevant regions of the phase space (Figure 2). To do so, a harmonic potential with constant $k = 5$ kcal/(mol Å^2) and center z_0 was applied to a single carbon atom located at the center of the particle. The value of k was chosen as it ensures a sufficient overlapping of the conformation space (Figures S2−S5). To maintain the slab of water at a fixed position along z, the bottommost layer of water molecules was frozen. For each pair of values (r_{OC}, r_{OH}) and for a given position z_0, data is averaged over three independent simulations (Figure S6). A total of 29 positions were explored, from $z_0 = -28$ to 28 Å, with the interface position located near $z = 0$. The exact position of the interface was determined from density profile analysis. Each simulation was performed for 1.2 ns, with the first 0.6 ns used as an equilibration step.

2.3. Simulation of Multiple GO Particles. In the case of multiple GO particle simulations, the system consists of a slab of liquid water with a number $N_w = 3300$ of water molecules in a box of dimensions $L_x \times L_y \times L_z = 4.8 \times 4.8 \times 10$ nm^3. In addition to the GO particle used for the PMF measurement, a number N of GO particles were initially positioned at the water−vapor interface. The N particles were initially aligned flat with the interface. Such configuration allows us to get insights into the formation of particle multilayers following the initial formation of a layer of GO particles at the fluid interface. The lateral dimensions of the system were chosen so that, when $N = 4$, the N particles initially form a thin layer covering the surface. For $4 < N < 8$, the particles form one full layer plus one partial layer on top of it. For $N = 8$, the particles form two full layers, and so on (see illustrations in the case $N = 10$ in Figures S8−S10). For each configuration, the degree of oxidation of the $N + 1$ particles was the same (same r_{OC} and same r_{OH}) but with randomized distribution. For each pair of values (r_{OC}, r_{OH}) and for a given position z_0 for the center of the harmonic potential, data is averaged over six independent simulations (Figure S7). A total of 15 positions were explored, from $z_0 = -28$ to 0 Å, with the interface position located near $z = 0$. Each simulation was performed for 2.2 ns, with the first 0.6 ns used as an equilibration step.

3. RESULTS AND DISCUSSION

3.1. Single GO Particle. We first extract the PMF for a single GO particle with a degree of edge functionalization $r_{OH} = 0.3$ and a degree of basal plane functionalization $r_{OC} = 0.05$ (Figure 3a). The PMF reaches a plateau for $z < -15$ Å, corresponding to the GO particle being into the water bulk phase, and another plateau for $z > 25$ Å, corresponding to the GO particle being into the vapor bulk phase (Figure 3d). In between the two plateaux, in $z = 0$, the PMF reaches a minimum that is located at the water−vapor interface. The exact position of the interface is chosen as the location where the time-averaged water density ρ equals half of the liquid bulk density ρ_{bulk} (Figure 3e). We define the adsorption energy ΔE_{ads} as

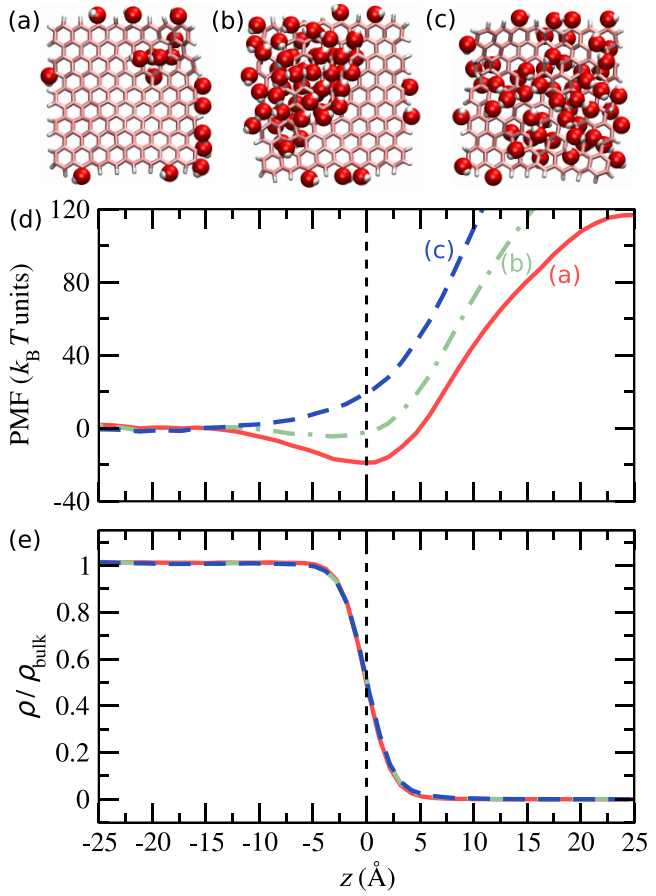

Figure 3. (a−c) GO particles with $r_{OH} = 0.3$ and $r_{OC} = 0.05$ (a) and $r_{OC} = 0.34$ (b, c). Oxygen groups at the basal plane in (c) are more evenly spread than in (b). (d) PMF as a function of z, for a GO particle with $r_{OH} = 0.3$ and $r_{OC} = 0.05$ (red full line), $r_{OC} = 0.34$ (green dot-dashed line), and $r_{OC} = 0.34$ with more evenly spread oxygen group at the basal plane (blue dashed line). The water−vapor interface is located at $z = 0$, with the liquid water in $z < 0$. (e) Water density ρ as a function of z and normalized by the liquid bulk density ρ_{bulk}.

$$\Delta E_{ads} = \mathrm{PMF}(z = 0) - \mathrm{PMF}(z \to -\infty) \quad (1)$$

Hence, $\Delta E_{ads} = (-23.7 \pm 3)\ k_B T$ for the GO particle of Figure 3a. A negative value for ΔE_{ads} indicates that the GO particle would favorably adsorb at the interface. The uncertainty on the value of ΔE_{ads} corresponds to the standard deviation calculated from the three independent simulations.

https://doi.org/10.1021/acs.langmuir.1c01902
Langmuir 2021, 37, 13322−13330

The adsorption energy was then measured for varying degrees of basal plane functionalization r_{OC} (r_{OC} = 0, 0.05, 0.17, 0.34, and 0.55 respectively) and fixed degree of edge functionalization r_{OH} = 0.3. Our results show that the absolute value of the adsorption energy ΔE_{ads} decreases monotonously for increasing the degree of basal plane functionalization r_{OC} (Figure 4a). In all five cases, the average value of ΔE_{ads} is

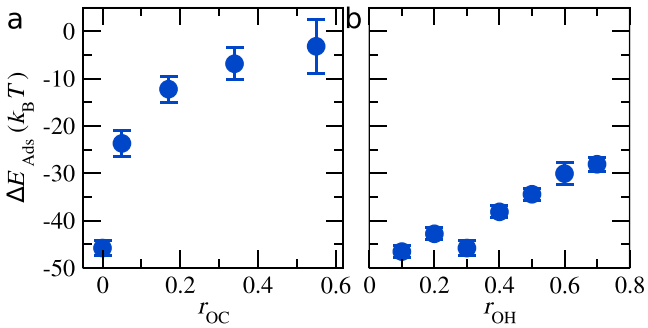

Figure 4. (a) Adsorption energy ΔE_{ads} as a function of the degree of surface oxidation r_{OC} for a single GO particle with a degree of edge oxidation r_{OH} = 0.3. (b) Adsorption energy ΔE_{ads} as a function of r_{OH} for a single GO particle with r_{OC} = 0.

negative. The adsorption energy was also measured for varying degrees of edge functionalization r_{OH} (r_{OH} = 0.1, 0.2, 0.3, 0.4, 0.5, 0.6, and 0.7, respectively) and fixed degree of surface functionalization r_{OC} = 0. Our results show that the absolute value of the adsorption energy ΔE_{ads} decreases quasilinearly for increasing values of r_{OH} (Figure 4b).

The results presented in Figure 4 reveal the importance of the distribution of oxygen groups on the absolute value of the adsorption energy $|\Delta E_{ads}|$. $|\Delta E_{ads}|$ decreases nonlinearly for increasing number of basal oxygen groups. However, $|\Delta E_{ads}|$ decreases quasilinearly for increasing the number of edge oxygen groups. As a consequence, a GO particle with r_{OC} = 0.17 and r_{OH} = 0.3 has a value for $|\Delta E_{ads}|$ that is higher that a GO particle with r_{OC} = 0 and r_{OH} = 0.7, despite having a lower number of oxygen groups; the number of oxygen groups is 17 (for r_{OC} = 0.17 and r_{OH} = 0.3) and 27 (for r_{OC} = 0 and r_{OH} = 0.7), respectively. These results highlight that oxygen groups distributed at the basal plane have a stronger influence on the adsorption energy as compared with oxygen groups distributed at the edge. Such impact of oxygen group positions on ΔE_{ads} can be understood as follows. Regardless of its position, the addition of a new oxygen group to a GO particle leads to a reduction of $|\Delta E_{ads}|$ as it increases the polarity of the GO particle. Such increased polarity increases the overall electrostatic interaction with water, which makes the GO particle more hydrophilic.[25] However, in the case where a new oxygen group is added to the basal plane of the GO particle, the surface area of pristine graphene patches is also reduced; these hydrophobic patches are known to control the amphiphilic character of the GO particle.[20]

The nonlinear dependence of ΔE_{ads} with r_{OC} suggested by our simulations is in stark contrast with what is typically assumed for Janus colloids.[36] In the modeling of adsorption of Janus colloids, one typically associates each homogeneous patch to a different surface energy density ("surface tension"). This approach invariably gives a linear dependence of the adsorption energy on the area of each chemically homogeneous patch. The fact that nonlinearities are observed in our simulation means that the effective surface energy of the oxygen-rich portion depends on its specific atomic structure in addition to its area.

The complexity of the relation between ΔE_{ads} and r_{OC} is even more striking when comparing two GO particles with the exact same number of oxygen groups but different surface distribution. A particle with r_{OC} = 0.34 and r_{OH} = 0.3 and oxygen group at the basal plane distributed in patches has a negative adsorption energy $|\Delta E_{ads}|$ (Figure 3b,d). However, a particle with oxygen groups at the basal plane more evenly spread (and the same values for r_{OC} and r_{OH}) has a positive adsorption energy (Figure 3c,d). These results indicate that only a particle with a "large enough" apparent surface of carbon atoms favorably adsorbs at a water−vapor interface, which is consistent with previous studies that showed that pristine graphene is surface active.[37]

The nanometric GO particles used in the present study contain typically only one hydrophilic patch on the basal plane, and therefore a particle with a relatively large fraction of surface groups is typically made of one hydrophilic and one hydrophobic parts, as seen in Figure 3b. As a consequence, such a particle tends to adopt a curved shape when adsorbed at the interface, with its hydrophobic part lying almost flat on the water−vapor surface, and its hydrophilic part maintained inside the liquid (Figure 5). In that case, the bending of the

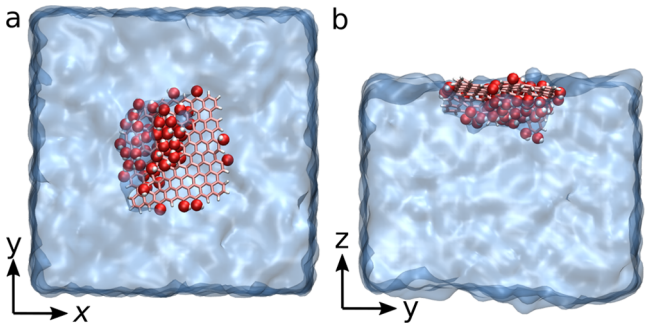

Figure 5. Snapshots of the molecular dynamics system with a single GO particle with r_{OC} = 0.34 and r_{OH} = 0.3. Panels show, respectively, the top view (a) and the lateral view (b). Water is represented as a continuum field.

particle is associated with an energy cost. By contrast, GO particles with a lower degree of oxidation at the basal plane, such as the particle in Figure 3a, are found to lie flat on the water−vapor surface.

One could develop a simple model to predict the occurrence of local bending deformations. Bending occurs when the moment of the force produced by the interface on the particle becomes comparable to the particle's bending rigidity. The force normal to the interface on the particle can be estimated as $F \simeq |\Delta E|/l$, where $l \simeq$ 0.5 nm is the force range (estimated here as half the molecular thickness of the interface obtained from density profiles) and $|\Delta E| \simeq 45/2 = 22.5\ k_BT$ is the adsorption energy of a patch of graphene of area half that of the entire nanosheet. The lever arm of this force is a patch correlation length ξ_c, characterizing the distance between the centers of the quasi-homogeneous carbon and oxygen-rich patches. Using for ξ_c half the particle length, the bending moment $F \times \xi_c$ is 45 k_BT. This value is comparable to the bending energy of pure graphene ($\approx$40−80 k_BT)[38] so our model, although crude, captures the right order of magnitude.

https://doi.org/10.1021/acs.langmuir.1c01902
Langmuir 2021, 37, 13322−13330

The estimated bending moment is much larger than that of a macroscopic sheet of GO ($\approx 1\ k_BT$),[38] but this is expected, as the measured bending rigidity of a GO sheet is an effective quantity accounting for many patches and material defects, while we are examining a truly nanoscopic deformation. The model indicates that an important role is played by the ratio of ξ_c and the particle lateral size L. If $\xi_c \ll L$, as one would expect to be the case in most physical experiments, the bending moment could induce small undulations of scale x_c even if the particle, on a macroscopic scale L, appeared to be adsorbed flat on the interface.

Finally, the impact of the type of oxygen groups on the adsorption energy was evaluated by measuring ΔE_{ads} for a GO particle with a surface covered with epoxide groups (r_{OC} = 0.17) and with edges terminated with hydroxyl groups (r_{OH} = 0.3). Our results give $\Delta E_{ads} = (-6.6 \pm 2.5)\ k_BT$, a higher (or less negative) value as compared with the results obtained with a GO particle with the same number of hydroxyl groups: $\Delta E_{ads} = (-12.2 \pm 2.7)\ k_BT$. The adsorption energy ΔE_{ads} was also measured in the case of a GO particle with edges terminated with carboxyl groups (r_{OH} = 0.3) and in the absence of surface groups (r_{OC} = 0). Our results give $\Delta E_{ads} = (-12.5 \pm 3)\ k_BT$, a higher (or less negative) value as compared with the results obtained with a GO particles with the same number of hydroxyl groups: $\Delta E_{ads} = (-45.8 \pm 1.5)\ k_BT$. These results indicate that GO particles covered with epoxide groups at the basal plane and/or carboxyl groups at the edges are less surface active than particles covered with the same number of hydroxyl groups, respectively. Therefore, the type of oxygen groups is another important parameter that controls the value of the adsorption energy of GO.

While developing a simple thermodynamic model for the case in which the basal plane contains oxygen groups is challenging, some simple considerations can be made for the case r_{OC} = 0. When the platelet is fully immersed in the bulk fluid, the basal plane of the solid is in contact with the liquid over an area $2\mathcal{A}$, where $\mathcal{A}$ is the basal plane area of the sheet excluding the edge area. Assuming a rigid platelet, the total energy associated with the particle completely immersed in the bulk fluid, E_{bulk}, is given by the sum of the liquid−solid interfacial energy, the interfacial energy of the flat liquid−vapor interface, and the energy, here denoted as E^{edge}_{bulk}, associated with the edges when they are completely immersed in the liquid:

$$E_{bulk} = 2\gamma_{ls}\mathcal{A} + \gamma_{lv}\mathcal{A}_\infty + E^{edge}_{bulk} \tag{2}$$

Here, γ_{ls} and γ_{lv} are the liquid−solid and liquid−vapor surface energy densities, respectively, and $\mathcal{A}_\infty$ is the total area of the liquid−vapor interface. When the platelet is embedded in the fluid interface, lying flat on it, a surface area $\mathcal{A}$ of the solid in contact with the liquid is replaced by a corresponding amount of the solid−vapor area. In addition, the liquid−vapor area is reduced by an amount $\mathcal{A}$ corresponding to the "hole" created in the interface by the particle. Hence, the total energy associated with the particle embedded in the fluid interface is

$$E_{interface} = \gamma_{ls}\mathcal{A} + \gamma_{sv}\mathcal{A} + \gamma_{lv}(\mathcal{A}_\infty - \mathcal{A}) + E^{edge}_{interface} \tag{3}$$

where $E^{edge}_{interface}$ is the edge energy and γ_{sv} is the solid−vapor surface energy density. If the particle adsorbs at the interface, then $E_{interface} < E_{bulk}$. The magnitude of the adsorption energy is given by

$$E_{bulk} - E_{interface} = (\gamma_{lv} - \Delta\gamma)\mathcal{A} + E^{edge}_{bulk} - E^{edge}_{interface} \tag{4}$$

where $\Delta\gamma = \gamma_{sv} - \gamma_{ls}$ is the difference between solid−vapor and liquid−solid surface energy densities. This quantity can be related to the contact angle θ through $\Delta\gamma = \gamma_{lv}\cos\theta$, hence

$$E_{bulk} - E_{interface} = \gamma_{lv}(1 - \cos\theta)\mathcal{A} + E^{edge}_{bulk} - E^{edge}_{interface} \tag{5}$$

Now, the contact angle of water deposited on flat graphene is larger than 90°,[39] thus $\cos\theta < 0$. If the edge energy terms were neglected, the adsorption energy per unit area would be slightly larger than $\gamma_{lv}A$ (typical values for pristine graphene suggest $\cos\theta \ll 1$). However, this prediction is in contrast with our MD observations, which show $(E_{bulk} - E_{interface})/\mathcal{A} < \gamma_{lv}$: for γ_{lv} = 63 mN/m,[40] a value appropriate for our simulation, we get $\gamma_{lv}\mathcal{A} \simeq 61\ k_BT$, while the magnitude of the adsorption energy for r_{OH} = 0 is about 45 k_BT (Figure 4a). Based on this simple thermodynamic model, the only way to explain our MD results is if the edge energy $E^{edge}_{interface}$ of the platelet in the interface is sufficiently large in comparison to E^{edge}_{bulk}. From our data, assuming $\theta \simeq 100°$[39] and γ_{lv} = 63 mN/m,[40] we get that $E^{edge}_{interface} - E^{edge}_{bulk}$ should be at least as large as 28.7 k_BT to match the observed adsorption energy obtained at zero basal plane coverage by oxygen groups. For large particles, we expect the edge energy to be subdominant with respect to the term $\gamma_{lv}(1 - \cos\theta)\mathcal{A}$, as the area grows as the square of the particle lateral size, while the length of the edges increases linearly with the particle size.

In summary, our results have shown that both the organization of oxygen groups at the GO particle surface (and more particularly at the GO particle basal plane) and the type of oxygen groups strongly impact the value of the adsorption energy of a single GO particle. However, experiments as well as potential applications are likely to be made in a limit of significant surface coverage, and it is therefore important to explore how particle−particle interactions influence the adsorption of GO particles at interfaces. In particular, an important question is which adsorption mechanisms set the thickness of GO layers at the fluid interface. In the next section, the adsorption energy of a test GO particle will be measured in the presence of a number N of GO particles.

3.2. Multiple GO Particles. Using a similar procedure as the one used for the single GO particle case, the PMF was measured for a test GO particle in a system made of a number N of GO particles initially disposed at the liquid−vapor interface, with N = 2, 4, 6, 8, and 10 (the total number of GO particles in the system is then N + 1). Snapshots of the molecular dynamics system with N = 4, r_{OC} = 0.05, and r_{OH} = 0.3 are shown in Figure 6 (see also Figures S8−S10 in the Supporting Information (SI)). The corresponding PMF is given by the full red line in Figure 7a and compared to the case of a single GO particle (N = 0) (dash-dotted black line in Figure 7a). Our results indicate that the adsorption energy is larger (in absolute value) in the case N = 4 as compared to the case N = 0, with $\Delta E_{ads} = (-60 \pm 5)\ k_BT$ for N = 4 and $\Delta E_{ads} = (-23.7 \pm 3)\ k_BT$ for N = 0. The water density profile is also slightly modified by the presence of multiple GO particles (Figure 7b).

The adsorption energy ΔE_{ads} of a test GO particle was then measured for different numbers of particles N (N = 2, 4, 6, 8, and 10) and r_{OC} = 0.05 and r_{OH} = 0.3 (red disks in Figure 8). Our results show that the adsorption energy ΔE_{ads} varies non-monotonously with N, with a minimum (in absolute value) in

https://doi.org/10.1021/acs.langmuir.1c01902
Langmuir 2021, 37, 13322−13330

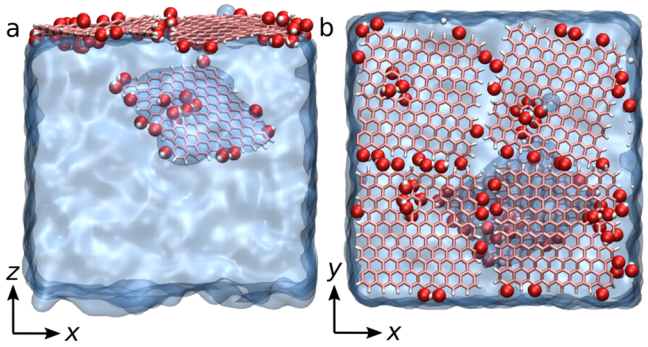

Figure 6. Snapshots of the molecular dynamics system with a number $N = 4$ of GO particles plus a test particle. GO particles have a degree of oxidation at the edge $r_{OH} = 0.3$ and a degree of oxidation at the basal plane $r_{OC} = 0.05$. Panels show, respectively, the lateral view (a) and the top view (b). Water is represented as a continuum field.

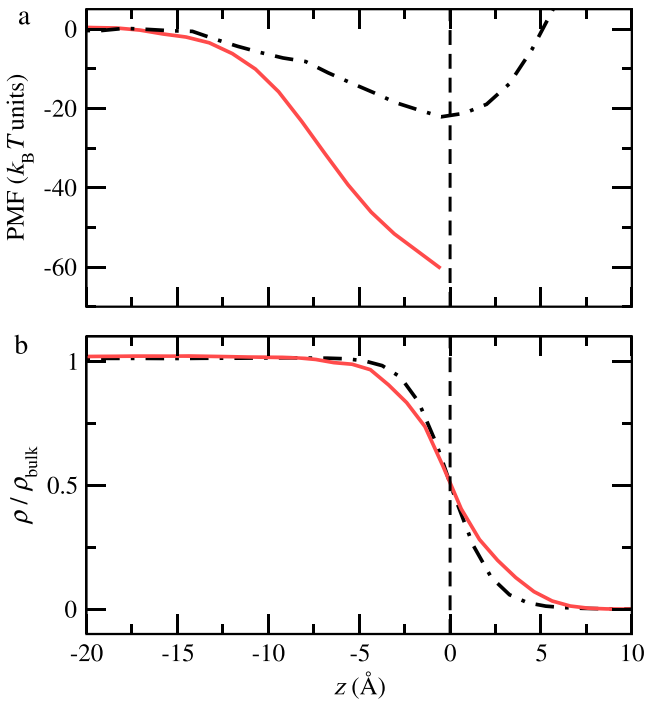

Figure 7. (a) PMF as a function of z, for GO particles with $r_{OC} = 0.05$ and $r_{OH} = 0.3$. The black dash-dotted line is the single-particle case, and the full red line is the multiple particle case with $N = 4$. The water−vapor interface is located at $z = 0$, with the liquid water in $z < 0$. (b) Water density ρ as a function of z and normalized by the liquid bulk density ρ_{bulk}.

$N = 2$. For $N \geq 4$ (and $r_{OC} = 0.05$ and $r_{OH} = 0.3$), the absolute value of ΔE_{ads} is larger than in the single-particle case ($N = 0$) and does not vary significantly with N. Similar simulations were performed in the case of GO particles without basal oxidation; $r_{OC} = 0$ and $r_{OH} = 0.3$. Similar to the $r_{OC} = 0.05$ case, ΔE_{ads} varies non-monotonously with N (black triangles in Figure 8), with a minimum (in absolute value) for $N = 2$ and a maximum for $N = 10$. Finally, simulations were performed for GO particles with $r_{OC} = 0.34$ and $r_{OH} = 0.3$. In that case, ΔE_{ads} is positive for $N \geq 2$ and negative only in the single-particle case $N = 0$ (blue squares in Figure 8).

Our results obtained in the case of multiple GO particles indicate that the effect of particle−particle interactions on the adsorption energy of a test GO particle depends notably on the

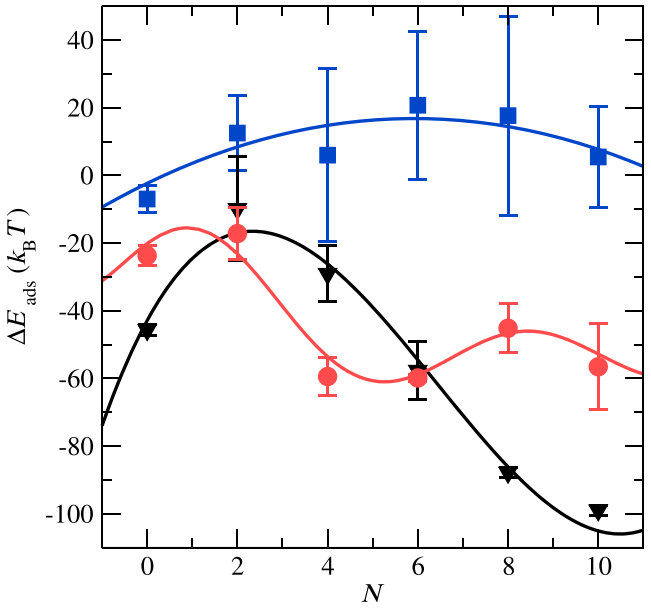

Figure 8. Adsorption energy ΔE_{ads} of a test GO particle as a function of the number N of GO particles at the water−vapor interface. GO particles have a degree of oxidation at the edge $r_{OH} = 0.3$, and a degree of oxidation at the basal plane $r_{OC} = 0$ (black triangles), $r_{OC} = 0.05$ (red disks), and $r_{OC} = 0.34$ (blue squares), respectively. Lines are guides to the eyes.

degree of basal oxidation of the particles. For GO particles with a large degree of basal oxidation (blue squares in Figure 8), the presence of a number $N > 0$ of GO particles at the interface makes it unfavorable for the test particle to adsorb. As a consequence, our results suggest that there is a maximum amount of GO particles that would favorably adsorb at the water−vapor interface. For the present system, the maximum number of (total) particles that would favorably adsorb at the interface is between one and three. In other words, for $r_{OC} = 0.34$, adsorption of GO particles is expected only as long as the surface density in particles remains low enough to prevent a direct contact between the GO particles at the interface. These results are consistent with the fact that GO particles with a large degree of basal oxidation are relatively hydrophilic and do not tend to form clusters when dispersed in water.[23]

For GO particles with a low or a zero degree of basal oxidation (respectively, red disks and black triangles in Figure 8), nonlinearities of ΔE_{ads} as a function of N are found, with the adsorption of the test particle being the less favorable for $N = 2$ and the most favorable for largest values of N. We link these nonlinearities with the tendency of pristine graphene to form clusters in bulk water as well as at the interface between water and vapor.[41] By forming clusters, graphene particles reduce the contact area with water while increasing the more energetically favorable graphene−graphene contact.[42,43] However, such a simple picture does not account for minimums of $|\Delta E_{ads}|$ for $N = 2$. To understand this minimum at $N = 2$, one has to keep in mind that the lateral size of the particles used in the present study is equal to 2 nm. Therefore, a stack formed by all three GO particles in the case $N = 2$ has an effective thickness of $2\, d_{CC} + 2\xi \approx 1.2$ nm, where $d_{CC} = 3.35$ Å[44] is the interlayer distance and $\xi = 2.5$ Å[45,46] is the effective radius of the carbon atoms in water. Such parallelepiped rectangle of approximate dimensions $2 \times 2 \times 1.2$ nm^3 must expose a relatively large portion of its edges to the vapor phase (Figure

https://doi.org/10.1021/acs.langmuir.1c01902
Langmuir 2021, 37, 13322−13330

9a), which is energetically unfavorable as suggested by single-particle measurement (see the large positive value of PMF ($z \to \infty$) in Figure 3). In the case $N = 8$, however, GO particles are assembled essentially in two superimposed layers, each of them covering the entire lateral extent of the computational domain (Figure 9b). In this case, only the top surface of the top layer is exposed to vacuum and all of the edges of the GO particles are in contact with the more energetically favorable water or neighbor GO particles.

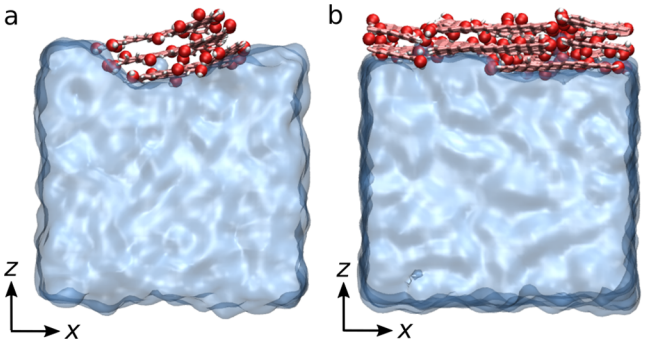

Figure 9. Snapshots of the molecular dynamics system with numbers $N = 2$ (a) and $N = 8$ GO particles plus a test particle. GO particles have a degree of oxidation at the edge $r_{OH} = 0.3$ and a degree of oxidation at the basal plane $r_{OC} = 0$. Water is represented as a continuum field.

3.3. Discussion. One important implication of our results is that the adsorption behavior in the case of multiple GO particles cannot be predicted from adsorption energy measurement obtained in the case of a single GO particle, at least for the relatively crowded surfaces we consider here. One reason for that are the strong interactions between GO particles, and in particular, the tendency of GO particles with a low degree of basal oxidation to form clusters and stack when in suspension. Particle–particle interactions and clustering strongly modify the value of the adsorption energy of a single particle, and, depending on the degree of oxidation of the GO particles, may either favor or hinder the adsorption of new particles at the interface. To properly predict such complex effects, one needs to develop models accounting for changes in solid–solid, solid–liquid, and liquid–vapor surface energies at the two-particle level at least, as well as the chemical heterogeneities and large aspect ratio of GO particles. Such analysis is beyond the scope of the present article but will have to be conducted in future works.

In the present study, molecular simulations have been chosen as they offer a good description of interactions between GO and water, including for instance the atomic details of oxygen surface groups. However, one major limitation of such atomic simulations is the size of the system, with simulation boxes (and consequently GO particles) being limited to nanometer sizes. The GO nanoparticles used in this study are made of a small number of hydrophilic/hydrophobic patches (typically one hydrophilic and one hydrophobic patches in our case), while common GO particles are micrometric in size and made of a large number of patches. Such a difference between simulations and experiments makes it difficult to extrapolate atomistic results to macroscopic scales. Another obstacle encountered when performing molecular simulations is the small time scales accessible, typically a few nanoseconds. Such time scales are sufficient to study the adsorption of a single GO particle of a few nanometers since the typical rotational diffusion coefficient of a GO particle with half length $a = 1$ nm is $D_r = 3\ k_B T/32\ \eta a^3 \approx 0.4\ \mathrm{ns}^{-1}$ (here, we use the formula for a thin disk of zero thickness[47]). However, the formation of clusters is associated with relaxation times that are larger than the duration of a typical molecular simulation, and our simulations in the case of multiple particles do not allow for an efficiently sampling of the configuration space. To overcome this difficulty, each simulation was reproduced multiple times using different initial positions for the N GO particles of the layer (see Figures S8–S10). Future numerical work should focus on using computational methods that allow for the exploration of larger times and larger scales, such as coarse-grained modeling or continuum calculations. The loss of precision inherent with such methods, as compared to all-atoms molecular dynamics, could be overcome in part using molecular dynamics results as a basis for calibrating the simulations, as is done in ref 48.

The dynamics of particle–particle interaction is an important aspect that is not accounted for by our present free-energy calculations. Understanding the dynamics of particle agglomeration and stacking is crucial as it can explain certain differences between numerical and experimental observations. For instance, in the case of pristine graphene, the typical stacking time for particles trapped at a water–vapor interface was found to increase exponentially with the contact edge length of the particles.[41] Therefore, stacking is more likely to be observed with nanometric particles during molecular dynamics simulations than it is during experiments that typically involve micrometric particles.[41,49] In the case of GO, oxygen groups at the edges and basal plane of the particles are known to affect the particle–particle energy of interactions,[50] and therefore, their presence is expected to lead to a different stacking time compared to the one measured with pristine graphene.

4. CONCLUSIONS

In this article, we used all-atom molecular simulations to study the adsorption of single and multiple GO nanoparticles at the interface between water and vapor. The adsorption energy in the case of a single GO particle was found to vary nonlinearly with the basal plane coverage r_{OC}. Our results show that these nonlinearities are due to the size of hydrophobic surface patches at the particle basal plane. Consequently, GO particles with oxygen groups distributed in patches were found to have a larger adsorption energy (in absolute value) than particles with uniformly spread oxygen groups. Our results obtained in the case of multiple GO particles at the interface highlight the significance and the complexity of particle–particle interactions on adsorption behavior. Two different regimes were identified, depending on the value of r_{OC}. For low r_{OC} (i.e., rather hydrophobic particles), particle–particle interactions were found to lead to an increase in the absolute value of the adsorption energy of a test particle, which we attribute to the tendency of hydrophobic GO particles to form clusters at a water–vapor interface. For the high r_{OC} value, however, particle–particle interactions limit the adsorption of new particles at the interface. Our results suggest that for high r_{OC} values, the adsorption of GO particles would be mildly favorable in the very dilute regime only because in this regime a direct contact between GO particles is statistically unlikely.

https://doi.org/10.1021/acs.langmuir.1c01902
Langmuir 2021, 37, 13322–13330

■ ASSOCIATED CONTENT

Supporting Information

The Supporting Information is available free of charge at https://pubs.acs.org/doi/10.1021/acs.langmuir.1c01902.

Single GO particle with L = 2 nm, r_{OH} = 0.3, and r_{OC}= 0.17 (Figure S1); set of histograms corresponding to a simulation with a single GO particle with r_{OH} = 0.3 and r_{OC} = 0.34 (Figure S2); set of histograms corresponding to a simulation with multiple GO particles with N = 4, r_{OH} = 0.3, and r_{OC} = 0.34 (Figure S3); set of histograms corresponding to a simulation with multiple GO particles with N = 4, r_{OH} = 0.3, and r_{OC} = 0.05 (Figure S4); error on the value of ΔE as a function of the data acquisition duration for a single GO particle with r_{OH} = 0.3 and r_{OC} = 0 (Figure S5); PMF for a single GO particle with r_{OH} = 0.3 and r_{OC} = 0.17 (Figure S6); PMF in the case of multiple GO particles with r_{OH} = 0.3, r_{OC} = 0.05, and N = 8 (Figure S7); example 1/3 of a system of multiple GO particles, with N = 10, r_{OC} = 0.05, and r_{OH} = 0.3 (Figure S8); example 2/3 of a system of multiple GO particles, with N = 10, r_{OC} = 0.05, and r_{OH} = 0.3 (Figure S9); and example 3/3 of a system of multiple GO particles, with N = 10, r_{OC} = 0.05, and r_{OH} = 0.3 (Figure S10) (PDF)

■ AUTHOR INFORMATION

Corresponding Author

Lorenzo Botto − *Process and Energy Department, 3ME Faculty of Mechanical, Maritime and Materials Engineering, TU Delft, Delft 2628 CD, The Netherlands*; Email: l.botto@tudelft.nl

Author

Simon Gravelle − *School of Engineering and Material Science, Queen Mary University of London, London E1 4NS, United Kingdom*; orcid.org/0000-0003-2149-6706

Complete contact information is available at: https://pubs.acs.org/10.1021/acs.langmuir.1c01902

Notes

The authors declare no competing financial interest.

■ ACKNOWLEDGMENTS

This project has received funding from the European Research Council (ERC) under the European Union's Horizon 2020 research and innovation programme (Grant Agreement No. 715475). This research utilized Queen Mary's Apocrita HPC facility, supported by QMUL Research-IT. The authors thank M. Stojanova for comments on the manuscripts.

■ REFERENCES

(1) *Particles at Fluid Interfaces and Membranes: Attachment of Colloid Particles and Proteins to Interfaces and Formation of Two-Dimensional Arrays*; Kralchevsky, P. A.; Nagayama, K., Eds.; Elsevier, 2001; Vol. *10*, p 654.

(2) Hunter, T. N.; Pugh, R. J.; Franks, G. V.; Jameson, G. J. The role of particles in stabilising foams and emulsions. *Adv. Colloid Interface Sci.* **2008**, *137*, 57−81.

(3) Binks, B. P. Colloidal Particles at a Range of Fluid-Fluid Interfaces. *Langmuir* **2017**, *33*, 6947−6963.

(4) Fei, W.; Gu, Y.; Bishop, K. J. Active colloidal particles at fluid-fluid interfaces. *Curr. Opin. Colloid Interface Sci.* **2017**, *32*, 57−68.

(5) Imperiali, L.; Clasen, C.; Fransaer, J.; Macosko, C. W.; Vermant, J. A simple route towards graphene oxide frameworks. *Mater. Horiz.* **2014**, *1*, 139−145.

(6) Park, B. J.; Lee, D. Particles at fluid-fluid interfaces: From single-particle behavior to hierarchical assembly of materials. *MRS Bull.* **2014**, *39*, 1089−1096.

(7) Jiang, H.; Sheng, Y.; Ngai, T. Pickering emulsions: Versatility of colloidal particles and recent applications. *Curr. Opin. Colloid Interface Sci.* **2020**, *49*, 1−15.

(8) Tang, T.-Y.; Zhou, Y.; Arya, G. Interfacial Assembly of Tunable Anisotropic Nanoparticle Architectures. *ACS Nano* **2019**, *13*, 4111−4123.

(9) Botto, L.; Lewandowski, E. P.; Cavallaro, M.; Stebe, K. J. Capillary interactions between anisotropic particles. *Soft Matter* **2012**, *8*, 9957−9971.

(10) Park, B. J.; Lee, D. Equilibrium orientation of nonspherical Janus particles at fluid-fluid interfaces. *ACS Nano* **2012**, *6*, 782−790.

(11) Wei, P.; Luo, Q.; Edgehouse, K. J.; Hemmingsen, C. M.; Rodier, B. J.; Pentzer, E. B. 2D Particles at Fluid-Fluid Interfaces: Assembly and Templating of Hybrid Structures for Advanced Applications. *ACS Appl. Mater. Interfaces* **2018**, *10*, 21765−21781.

(12) Lee, S. H.; Kim, H. W.; Hwang, J. O.; Lee, W. J.; Kwon, J.; Bielawski, C. W.; Ruoff, R. S.; Kim, S. O. Three-Dimensional Self-Assembly of Graphene Oxide Platelets into Mechanically Flexible Macroporous Carbon Films. *Angew. Chem.* **2010**, *122*, 10282−10286.

(13) Dreyer, D. R.; Park, S.; Bielawski, C. W.; Ruoff, R. S. The chemistry of graphene oxide. *Chem. Soc. Rev.* **2010**, *39*, 228−240.

(14) Cai, W.; Piner, R. D.; Stadermann, F. J.; Park, S.; Shaibat, M. A.; Ishii, Y.; Yang, D.; Velamakanni, A.; An, S. J.; Stoller, M.; An, J.; Chen, D.; Ruoff, R. S. Synthesis and Solid-State NMR Structural Characterization of 13C-Labeled Graphite Oxide. *Science* **2008**, *321*, 1815−1818.

(15) Yan, J. A.; Xian, L.; Chou, M. Y. Structural and electronic properties of oxidized graphene. *Phys. Rev. Lett.* **2009**, *103*, No. 086802.

(16) Erickson, K.; Erni, R.; Lee, Z.; Alem, N.; Gannett, W.; Zettl, A. Determination of the local chemical structure of graphene oxide and reduced graphene oxide. *Adv. Mater.* **2010**, *22*, 4467−4472.

(17) Yang, J.; Shi, G.; Tu, Y.; Fang, H. High Correlation between Oxidation Loci on Graphene Oxide. *Angew. Chem.* **2014**, *126*, 10354−10358.

(18) Kim, F.; Cote, L. J.; Huang, J. Graphene oxide: Surface activity and two-dimensional assembly. *Adv. Mater.* **2010**, *22*, 1954−1958.

(19) Kim, J.; Cote, L. J.; Kim, F.; Yuan, W.; Shull, K. R.; Huang, J. Graphene oxide sheets at interfaces. *J. Am. Chem. Soc.* **2010**, *132*, 8180−8186.

(20) Cote, L. J.; Kim, J.; Tung, V. C.; Luo, J.; Kim, F.; Huang, J. Graphene oxide as surfactant sheets. *Pure Appl. Chem.* **2010**, *83*, 95−110.

(21) Zhang, X.; Sun, H.; Yang, S. Self-limiting assembly of two-dimensional domains from graphene oxide at the air/water interface. *J. Phys. Chem. C* **2012**, *116*, 19018−19024.

(22) Huang, Q.-Q.; Wen, Y.-E.; Bai, H.; Zhang, Z.; Jiang, Y. Spontaneous Adsorption of Graphene Oxide on Multiple Polymeric Surfaces. *Langmuir* **2021**, *37*, 8829−8839.

(23) Luo, J.; Cote, L. J.; Tung, V. C.; Tan, A. T.; Goins, P. E.; Wu, J.; Huang, J. Graphene oxide nanocolloids. *J. Am. Chem. Soc.* **2010**, *132*, 17667−17669.

(24) Shih, C. J.; Lin, S.; Sharma, R.; Strano, M. S.; Blankschtein, D. Understanding the pH-dependent behavior of graphene oxide aqueous solutions: A comparative experimental and molecular dynamics simulation study. *Langmuir* **2012**, *28*, 235−241.

(25) Paulista Neto, A. J.; Fileti, E. E. Elucidating the amphiphilic character of graphene oxide. *Phys. Chem. Chem. Phys.* **2018**, *20*, 9507−9515.

(26) Plimpton, S. Fast Parallel Algorithms For Short-range Molecular-dynamics. *J. Comput. Phys.* **1995**, *117*, 1−19.

(27) Berendsen, H. J.; Grigera, J. R.; Straatsma, T. P. The missing term in effective pair potentials. *J. Phys. Chem. C* **1987**, *91*, 6269−6271.
(28) Jorgensen, W. L.; Maxwell, D. S.; Tirado-Rives, J. Development and Testing of the OLPS All-Atom Force Field on Conformational Energetics and Properties of Organic Liquids. *J. Am. Chem. Soc.* **1996**, *118*, 11225−11236.
(29) Ryckaert, J.-P.; Ciccotti, G.; Berendsen, H. J. Numerical integration of the cartesian equations of motion of a system with constraints: molecular dynamics of n-alkanes. *J. Comput. Phys.* **1977**, *23*, 327−341.
(30) Darden, T.; York, D.; Pedersen, L. Particle mesh Ewald: An N log(N) method for Ewald sums in large systems. *J. Chem. Phys.* **1993**, *98*, 10089−10092.
(31) Lu, Q.; Luo, R. A Poisson-Boltzmann dynamics method with nonperiodic boundary condition. *J. Chem. Phys.* **2003**, *119*, 11035−11047.
(32) Sinclair, R. C.; Coveney, P. V. Modeling Nanostructure in Graphene Oxide: Inhomogeneity and the Percolation Threshold. *J. Chem. Inf. Model.* **2019**, *59*, 2741−2745.
(33) Gao, Y.; Xu, D.; Cui, T.; Li, D. Stability of hydrogen-terminated graphene edges. *Phys. Chem. Chem. Phys.* **2021**, *23*, 13261−13266.
(34) Kumar, S.; Rosenberg, J. M.; Bouzida, D.; Swendsen, R. H.; Kollman, P. A. The weighted histogram analysis method for free-energy calculations on biomolecules. I. The method. *J. Comput. Chem.* **1992**, *13*, 1011−1021.
(35) Kästner, J. Umbrella sampling. *Wiley Interdiscip. Rev.: Comput. Mol. Sci.* **2011**, *1*, 932−942.
(36) Bradley, L. C.; Chen, W. H.; Stebe, K. J.; Lee, D. Janus and patchy colloids at fluid interfaces. *Curr. Opin. Colloid Interface Sci.* **2017**, *30*, 25−33.
(37) Goggin, D. M.; Samaniuk, J. R. Dynamics of pristine graphite and graphene at an air-water interface. *AIChE J.* **2018**, *64*, 3177−3187.
(38) Poulin, P.; Jalili, R.; Neri, W.; Nallet, F.; Divoux, T.; Colin, A.; Aboutalebi, S. H.; Wallace, G.; Zakri, C. Superflexibility of graphene oxide. *Proc. Natl. Acad. Sci. U.S.A.* **2016**, *113*, 11088−11093.
(39) Taherian, F.; Marcon, V.; van der Vegt, N. F.; Leroy, F. What is the contact angle of water on graphene? *Langmuir* **2013**, *29*, 1457−1465.
(40) Vega, C.; De Miguel, E. Surface tension of the most popular models of water by using the test-area simulation method. *J. Chem. Phys.* **2007**, *126*, No. 154707.
(41) Goggin, D. M.; Bei, R.; Anderson, R.; Gómez-Gualdrón, D. A.; Samaniuk, J. R. Stacking of Monolayer Graphene Particles at a Water-Vapor Interface. *J. Phys. Chem. C* **2021**, *125*, 7880−7888.
(42) Paton, K. R.; et al. Scalable production of large quantities of defect-free few-layer graphene by shear exfoliation in liquids. *Nat. Mater.* **2014**, *13*, 624−630.
(43) Gravelle, S.; Kamal, C.; Botto, L. Liquid exfoliation of multilayer graphene in sheared solvents: a molecular dynamics investigation. *J. Chem. Phys.* **2020**, *152*, No. 104701.
(44) Chung, D. D. L. Review Graphite. *J. Mater. Sci.* **2002**, *37*, 1475−1489.
(45) Gravelle, S.; Joly, L.; Ybert, C.; Bocquet, L. Large permeabilities of hourglass nanopores: From hydrodynamics to single file transport. *J. Chem. Phys.* **2014**, *141*, No. 18C526.
(46) Kamal, C.; Gravelle, S.; Botto, L. Hydrodynamic slip can align thin nanoplatelets in shear flow. *Nat. Commun.* **2020**, *11*, No. 2425.
(47) Sherwood, J. D. Resistance coefficients for Stokes flow around a disk with a Navier slip condition. *Phys. Fluids* **2012**, *24*, No. 093103.
(48) Williams, C. D.; Lísal, M. Coarse grained models of graphene and graphene oxide for use in aqueous solution. *2D Materials* **2020**, *7*, No. 025025.
(49) Goggin, D. M.; Zhang, H.; Miller, E. M.; Samaniuk, J. R. Interference Provides Clarity: Direct Observation of 2D Materials at Fluid-Fluid Interfaces. *ACS Nano* **2019**, *14*, 777−790.
(50) Paulista Neto, A. J.; Fileti, E. E. Impact of Edge Groups on the Hydration and Aggregation Properties of Graphene Oxide. *J. Phys. Chem. B* **2018**, *122*, 2578−2586.

https://doi.org/10.1021/acs.langmuir.1c01902
Langmuir 2021, 37, 13322−13330